

Large Scale Learning of General Visual Representations for Transfer

Alexander Kolesnikov*, Lucas Beyer*, Xiaohua Zhai*,
Joan Puigcerver, Jessica Yung, Sylvain Gelly, and Neil Houlsby

Google Research, Brain Team
Zürich, Switzerland
{akolesnikov, lbeyer, xzhai}@google.com
{jpuigcerver, jessicayung, sylvaingelly, neilhoulby}@google.com

Abstract. Transfer of pre-trained representations improves sample efficiency and simplifies hyperparameter tuning when training deep neural networks for vision. We revisit the paradigm of pre-training on large supervised datasets and fine-tuning the weights on the target task. We scale up pre-training, and create a simple recipe that we call Big Transfer (BiT). By combining a few carefully selected components, and transferring using a simple heuristic, we achieve strong performance on over 20 datasets. BiT performs well across a surprisingly wide range of data regimes — from 10 to 1M labeled examples. BiT achieves 87.8% top-1 accuracy on ILSVRC-2012, 99.3% on CIFAR-10, and 76.7% on the Visual Task Adaptation Benchmark (which includes 19 tasks). On small datasets, BiT attains 86.4% on ILSVRC-2012 with 25 examples per class, and 97.6% on CIFAR-10 with 10 examples per class. We conduct detailed analysis of the main components that lead to high transfer performance.

1 Introduction

Deep learning yields strong performance in many vision tasks. However, success usually requires a large amount of task-specific labeled training data. Training also requires a large amount of compute. These per-task data and compute requirements can make solving new tasks prohibitively expensive.

Transfer learning offers a solution: some task-specific data is replaced by a large amount of generic data. To perform transfer, one first pre-trains a network on a large generic dataset. Transfer of knowledge from pre-training to new tasks then usually entails initializing networks for subsequent tasks using the weights learned during pre-training. Good performance can then be attained with fewer downstream labeled examples. Transfer learning can also shift computational requirements upstream. Although the pre-training phase is expensive, downstream tasks often require fewer training iterations [37,12].

In this paper, we revisit this simple paradigm: pre-train on a large supervised source domain, and fine-tune the weights on the target domain. Many

* Equal contribution

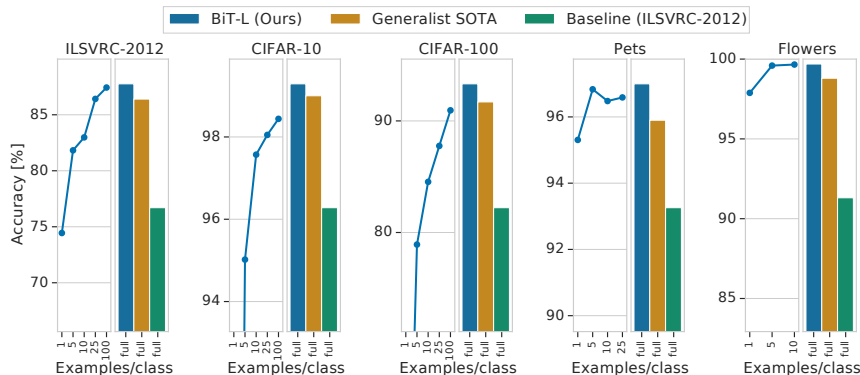


Fig. 1: Transfer performance of our pre-trained model, BiT-L, the previous state-of-the-art (SOTA), and a ResNet-50 baseline pre-trained on ILSVRC-2012 to downstream tasks. Here we consider only methods that are pre-trained independently of the final task (generalist representations), like BiT. The bars show the accuracy when fine-tuning on the full downstream dataset. The curve on the left-hand side of each plot shows that BiT-L performs well even when transferred using only few images (1 to 100) per class.

new techniques have been introduced to improve deep network training. Recent examples include: architectures such as EfficientNet [43] or ResNeXt [51]; optimization strategies such as Adam [23] and Cosine Annealing [30]; Stochastic Weight Averaging [20,1]; regularizers such as CutMix [53], MixUp [56], stochastic depth, and label smoothing [42]; and new normalization layers, such as Instance Normalization [47], Layer Normalization [2], and Group Normalization [49]. We distill from these the most effective techniques required to create a single model that can transfer to many tasks. We call such models “Big Transfer” (BiT).

We pre-train BiT-Large (BiT-L) on the JFT-300M dataset [40], which contains 300M noisily labelled images. BiT-L attains state-of-the-art performance on many visual classification tasks with training sets ranging from 10 to 1M examples (Figure 1). These tasks include ImageNet’s ILSVRC-2012 [8], CIFAR-10/100 [25], Oxford-IIIT Pet [35], Oxford Flowers-102 [34] (including low-data variants), and the 1000-sample VTAB-1k benchmark [55], which itself is composed of 19 diverse datasets. We also train BiT-M on the public ImageNet-21k dataset, and demonstrate large improvements compared to the conventional ILSVRC-2012 pre-training.

Importantly, BiT only needs to be pre-trained once. Subsequent fine-tuning to downstream tasks is cheap. This is in contrast to other state-of-the-art methods that require extensive training on support data conditioned on the task at hand [33,50,52]. Not only does BiT require a short fine-tuning protocol for each new task, but also BiT does not require extensive hyperparameter tuning on new tasks. We present a heuristic for setting the hyperparameters for transfer, which works well on many new tasks.

The goal of this paper is not to introduce a new component, or add further complexity to state-of-the-art deep learning pipelines. Instead, we aim to simplify, and create a pre-train/transfer pipeline which uses a minimal number of necessary tricks to attain very strong performance across a broad spectrum of popular classification tasks. We also study the effect of different components, and provide insight into the interplay between scale, architecture, and training hyperparameters. For practitioners, we plan to release a performant BiT-M model trained on the public ImageNet-21k dataset.

2 The Components of BiT

We review the components that we found necessary to build a pre-trained network that attains good performance across many tasks. These are divided into two groups: *upstream* — those used during pre-training, and *downstream* — those used for fine-tuning on a new task.

2.1 Upstream Pre-Training

The first component is scale. It is widely known that large architectures require large datasets to exhibit their benefits, and vice versa. We find that long training schedules are crucial for training with very large data. We train three BiT models on three large datasets: ILSVRC-2012 [38] which contains 1.3M images (BiT-S), ImageNet-21k [8] which contains 14M images (BiT-M), and JFT [40] which contains 300M images (BiT-L). We show that a long schedule is crucial to harness the benefits of larger datasets and models, see Section 4.2.

The second component is Group Normalization (GN) [49]. Batch Normalization (BN) [19] is a popular technique used to stabilize training, and is used in most state-of-the-art vision models. However, BN can hurt in transfer learning, likely due to the requirement to update running statistics. We study this empirically in Section 4.3. BN can also be detrimental when training with few images per chip, since batch statistics become too noisy. In that regime, GN, when combined with Weight Standardization (WS), is shown to improve performance on ImageNet and COCO [29]. We demonstrate that both GN and WS are effective at a larger batch size, and have a significant impact on transfer learning.

2.2 Transfer to Downstream Tasks

We propose a cheap fine-tuning protocol that applies to many diverse tasks, with training set sizes spanning many orders of magnitude. In particular, we avoid expensive hyperparameter search for every new task and dataset size. Our heuristic hyperparameter configuration—which we call BiT-hyperparam—selects the resolution, the use of MixUp [56], and the training schedule based on dataset characteristics; see Table 1 for details. With this strategy, BiT attains strong performance across over 20 tasks and training regimes ranging from 1

Table 1: The proposed hyperparameter selection strategy, BiT-hyperparam, that we use for all transfer runs in this paper. While it works well across tasks, one can get better performance with additional tuning, see Section 4.4.

Hyperparameter	Values
Optimizer	SGD, learning rate: 0.003, momentum: 0.9, batch size: 512
Resolution	<96 px: resize(160),crop(128) >96 px: resize(448),crop(384)
MixUp	<20 k samples: NO >20 k samples: YES
Training Steps	<20 k samples: 500 <500 k samples: 10 k >500 k samples: 20 k

example per class to large datasets. We give a high-level overview of our choices here and more detailed exposition in Section 3.3.

During fine-tuning, we use limited data pre-processing: we resize the image to a fixed square size, crop out a smaller random square, and randomly horizontally flip the image at training time. At test time, we only resize the image to a fixed size. The only per-task heuristic we apply is that we do not perform random horizontal flipping or cropping for tasks where doing so would destroy the label semantics, such as when predicting object orientations or coordinates in pixel space.

Recent work has shown that existing augmentation methods induce inconsistency between training and test resolutions for ConvNets [45]. A common heuristic is scaling up the resolution by a small factor at test time. A better solution, proposed by [45], is to introduce an additional step at which the trained model is fine-tuned to the test resolution. This fits well with transfer learning: we include the resolution change during our fine-tuning step.

MixUp [56] linearly interpolates between two image samples. The ground truth label of the new sample is given by the linear interpolation of one-hot labels. This technique has been used in many recent works, and similarly we found it can help during transfer.

Finally, we note that we do not use weight decay, neither towards zero, nor towards the pre-trained weights. We also do not use dropout. Despite the fact that the network is very large—BiT-L has about 1 billion parameters—the performance is surprisingly good without needing these techniques and their respective hyperparameters, even when transferring to very small datasets. We find that an appropriately chosen schedule is sufficient. The schedule is automatically chosen based on the number of samples, with larger datasets having longer schedules (see Table 1).

3 Experiments

We train three upstream models using three datasets of different scale: BiT-S, BiT-M, BiT-L. We evaluate these models on a wide range of downstream tasks that span high and low data regimes.

3.1 Data for upstream pre-training

BiT-S is trained on the popular ILSVRC-2012 variant of the ImageNet dataset. This dataset contains 1.28 million images and 1000 classes. Each image has a single label, and the labels are organized according to the WordNet hierarchy. BiT-M is trained on the full ImageNet-21k dataset [8], a publicly available dataset with 14.2 million images and 21k classes also organized using WordNet.

BiT-L is trained on the JFT-300M dataset, as in [40,33,50]. This dataset is a new version of that used in [16,6]. JFT-300M consists of around 300 million images with 1.26 labels per image on average. The labels are organized into a hierarchy of 18 291 classes. Annotation is performed using an automatic pipeline, and are therefore imperfect; approximately 20% of the labels are noisy.

3.2 Downstream tasks

We evaluate BiT on standard computer vision benchmarks: ILSVRC-2012 [8], CIFAR-10/100 [25], Oxford-IIIT Pet [35] and Oxford Flowers-102 [34]. These datasets have a long history and differ in the total number of images, input resolution and nature of their categories, from general object categories in ImageNet and CIFAR to fine-grained ones in Pets and Flowers. We always fine-tune BiT on the official training split and report results on the official *test* split if publicly available. Otherwise, we use the *val* split.

To further assess the generality of representations learned by BiT models, we leverage the recently introduced Visual Task Adaptation Benchmark (VTAB) [55] that consists of 19 visual tasks. For each task in VTAB, we have access to 1000 training samples (VTAB-1k variant). These tasks are organized into three groups: *natural*, *specialized* and *structured*. The VTAB-1k score is computed as the top-1 recognition performance averaged over these 19 tasks. The *natural* group of tasks represents classical tasks that contain natural images captured using standard cameras. The *specialized* group also contains images captured in the real world, but through specialist equipment, such as satellite or medical images. Finally, the *structured* tasks are mostly generated from simulated environments and assess understanding of the the structure of a scene. Example tasks are object counting and 3D depth estimation.

3.3 Hyperparameter Details

Upstream Pre-Training For all of our models, we use a vanilla ResNet-v2 architecture [14], except that we replace all Batch Normalization [19] layers with Group Normalization [49] and use Weight Standardization [36] in all convolutional layers. This change is analyzed in Section 4.3. The BiT-S and BiT-M models use the ResNet-101 architecture, where every hidden layer is widened by a factor of three (ResNet101x3). To benefit from the larger dataset, BiT-L uses a ResNet-152x4 model, which has 0.93 billion trainable parameters. We explore the coupling between the datasets and the size of the model in Section 4.1.

Table 2: Top-1 accuracy for BiT-L on many datasets using a single model and single hyperparameter setting per task (BiT-hyperparam). The entries show median \pm standard deviation across 5 fine-tuning runs. Specialist models are those that condition pre-training on each task, while generalist models, including BiT, perform task-independent pre-training.

	BiT-L	Generalist SOTA	Specialist SOTA
ILSVRC-2012	87.76 \pm 0.09	86.4 [45]	87.4 [50]
CIFAR-10	99.35 \pm 0.03	99.0 [17]	-
CIFAR-100	93.60 \pm 0.18	91.7 [43]	-
Pets	96.76 \pm 0.18	95.9 [17]	97.1 [33]
Flowers	99.69 \pm 0.01	98.8 [43]	97.7 [33]
VTAB (19 tasks)	76.65 \pm 0.11	71.7 [46]	-

We train both BiT-S and BiT-M for 90 epochs and decay the learning rate by a factor of 10 at 30, 60 and 80 epochs. For BiT-L, we train for 40 epochs with an initial learning rate of 0.03, with 5000 linear warmup steps and decay the learning rate after 10, 23, 30 and 37 epochs. We use a global batch size of 4096 and train on a Cloud TPUv3-512 [22], resulting in 8 images per chip. For optimization with large batch sizes we employ recipes from [9]. In particular, we use linear learning rate warmup for 5000 optimization steps and scale learning rate multiplicatively by $\frac{\text{batch size}}{256}$.

Downstream Fine-Tuning We desire a low per-task adaptation cost. We therefore run a single hyperparameter setting for each downstream task. However, due to different resolutions and dataset sizes, identical hyperparameters will not work well across all tasks. To address this we provide a heuristic setting, BiT-hyperparam, to determine all downstream hyperparameters. Of the hundreds of hyperparameter choices, BiT-hyperparam selects the most important based on the task’s image resolution and training set size.

The logic for BiT-hyperparam is summarized in Table 1. For all the tasks, we set the initial learning rate to 0.003 and batch size to 512. We resize input images smaller than 96×96 pixels to 160×160 pixels, and then take a random crop of 128×128 pixels. We resize larger images to 448×448 and take a 384×384 -sized crop for BiT-S and BiT-M. For BiT-L, we take a 480×480 crop out of 512×512 images. See Appendix B for more details about how we apply horizontal flips and random crops.

We define three task regimes: we call *small* tasks those with fewer than 20k labeled examples, *medium* those with fewer than 500k, and any larger dataset is a *large* task. We fine-tune BiT for 500 steps on small tasks, for 10k steps on medium tasks, and for 20k steps on large tasks. During fine-tuning, we decay the learning rate by a factor of 10 at 30%, 60% and 90% of the training steps. Finally, we use MixUp [56], with $\alpha = 0.1$, for medium and large datasets.

Table 3: Absolute accuracy (%) improvements of pre-training on the publicly available ImageNet-21k over the “standard” ILSVRC-2012. Both models use the ResNet101x3 architecture.

	ILSVRC- 2012	CIFAR- 10	CIFAR- 100	Pets	Flowers	VTAB-1k (19 tasks)
BiT-S (ILSVRC-2012)	80.33	97.16	85.30	93.70	91.03	69.39
BiT-M (ImageNet-21k)	84.45	98.48	88.66	94.57	99.48	72.52
Improvement	+4.12	+1.32	+3.36	+0.87	+8.45	+3.13

3.4 Evaluation on Standard Computer Vision Benchmarks

We evaluate BiT-L on standard benchmarks and compare its performance to the current state-of-the-art results (Table 2). Here we separate models that perform task-independent large-scale pre-training (“general” representations), from those that perform task-dependent large-scale pre-training (“specialist” representations). The specialist methods condition on a particular task, for example ILSVRC-2012, then train using a large support dataset, such as JFT-300M [33] or Instagram-1B [52]. Further details are discussed in Section 5. Specialist representations are highly effective, but require a large training cost *per task*. By contrast, generalized representations require large-scale training *only once*, followed by a cheaper adaptation phase.

BiT-L outperforms previously reported generalist SOTA models, and in almost all cases, specialist models. BiT-L model achieves these results without extensive hyperparameter tuning for each individual dataset: we use BiT-hyperparam for all our runs (including 19 VTAB tasks) and do not perform costly tuning.

Inspired by strong results of BiT-L trained on the in-house JFT-300M dataset, we draw our attention towards the public ImageNet-21k dataset. This dataset is more than 10 times bigger than the widely used ILSVRC-2012, but is mostly overlooked by the research community. In Table 3 we demonstrate that BiT-M trained on ImageNet-21k leads to substantially improved visual representations compared to the same model trained on ILSVRC-2012 (BiT-S), as measured by all our benchmarks.

In our detailed analysis, in particular in Section 4.2, we discuss pitfalls that may have hindered wide adoption of ImageNet-21k as a dataset model for pre-training and highlight crucial components of BiT that enabled success on this large dataset.

3.5 Evaluation On Low-data Regime

In this section we study how many labeled samples are needed to effectively transfer BiT-L to a new downstream task. To this end, we fine-tune our model on small subsets of downstream training data. We test BiT-L in a low data

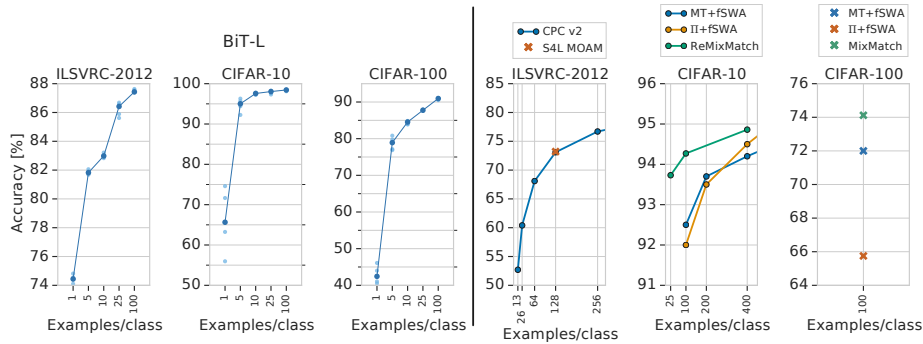


Fig. 2: Experiments in the low data regime. **Left:** Transfer performance of BiT-L. Each point represents the result after training on a balanced random subsample of the dataset (5 trials/subsamples per dataset). The median across these runs is highlighted with the curves. With one image per class, the variance is large but it shrinks rapidly as the number of examples/class increases. **Right:** We summarize the state of the art in semi-supervised learning as reference points. Note that a direct comparison is not meaningful; although semi-supervised learning has access to unlabelled data from the same distribution, it does not make use of external labeled training data.

regime on a broad set of tasks, including ILSVRC-2012, CIFAR-10, and CIFAR-100 datasets and the recently introduced VTAB-1k that consists of 19 different downstream tasks.

Note that the goal here is similar to that in semi-supervised learning — in both cases, we want to attain high performance using fewer examples per class. Importantly, we use extra labelled out-of-domain data, whereas many of these methods leverage extra unlabelled in-domain data, so the results are not directly comparable. Nevertheless, it is interesting to compare relative benefits of leveraging generic labelled out-of-domain data versus unlabelled in-domain data.

Figure 2 (left half) shows how performance of BiT-L on ILSVRC-2012, CIFAR-10, and CIFAR-100 depends on the number of available labelled samples per class. Multiple points with the same amount of training data correspond to different random data subsamples (we evaluate 5 random subsamples for each examples-per-class configuration). Surprisingly, even with very few samples per class, BiT-L demonstrates strong performance and quickly approaches performance of the full-data regime. In particular, with just 1 labeled sample per class it achieves top-1 accuracy of 74.3% on ILSVRC-2012 and with 25 samples the top-1 accuracy goes to 86.4%. On the CIFAR-100 dataset, we achieve 85.0% with just 10 samples per class.

For reference, on the right side of Figure 2, we show the results from the semi-supervised learning community. Even though the results are not directly comparable, one can assess relative benefits of both approaches.

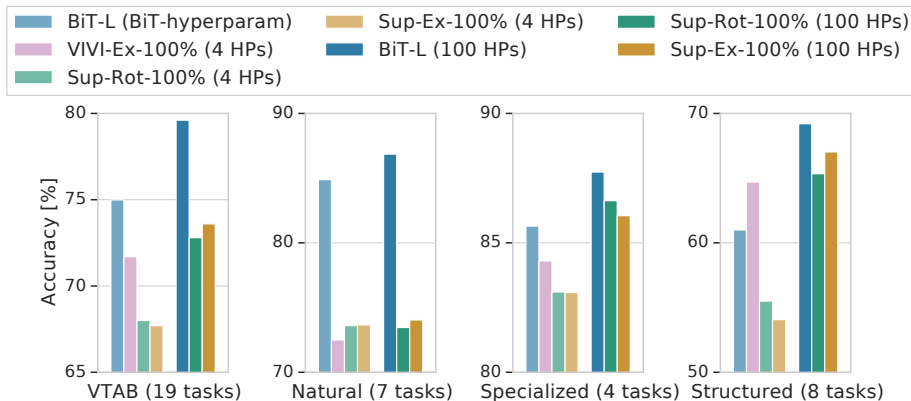


Fig. 3: Results on VTAB (19 tasks) with 1000 examples/task, along with the current SOTA. The light-colored bars compare various methods that sweep few hyperparameters per task: either four hyperparameters in previous work (“4 HPs”) or the single BiT-hyperparam. The dark bars compare the results of an extensive hyperparameter search (“100 HPs”), see Section 4.4.

Further, Figure 3 shows the performance of BiT-L on VTAB-1k that consists of 19 downstream tasks with only 1000 training samples for each task. Overall, BiT-L with BiT-hyperparam outperforms the previously reported state-of-the-art on VTAB-1k [46]. When looking into performance of VTAB-1k task subsets, our model is the best on *natural* and *specialized* tasks. However, the recently-proposed VIVI-Ex-100% [46] model that employs video-data during upstream training shows better results on the *structured* tasks.

For completeness, in Figure 3 we also evaluate our model with the extensive hyperparameter tuning during the fine-tuning stage. This leads to further performance improvements, see Section 4.4 for more analysis.

4 Detailed Analysis

In this section we perform detailed analysis of various components of BiT. In particular, we demonstrate the importance of model capacity, discuss practical optimization caveats, choice of normalization layer, and hyperparameter selection. We also analyze the effect of potential image duplication between upstream datasets used for pre-training and downstream test sets used for evaluation.

4.1 Big Models and Big Data

The general consensus is that larger models result in better upstream and downstream performance [24]. To investigate the effects of model capacity and upstream dataset size on downstream performance, we train different ResNet ar-

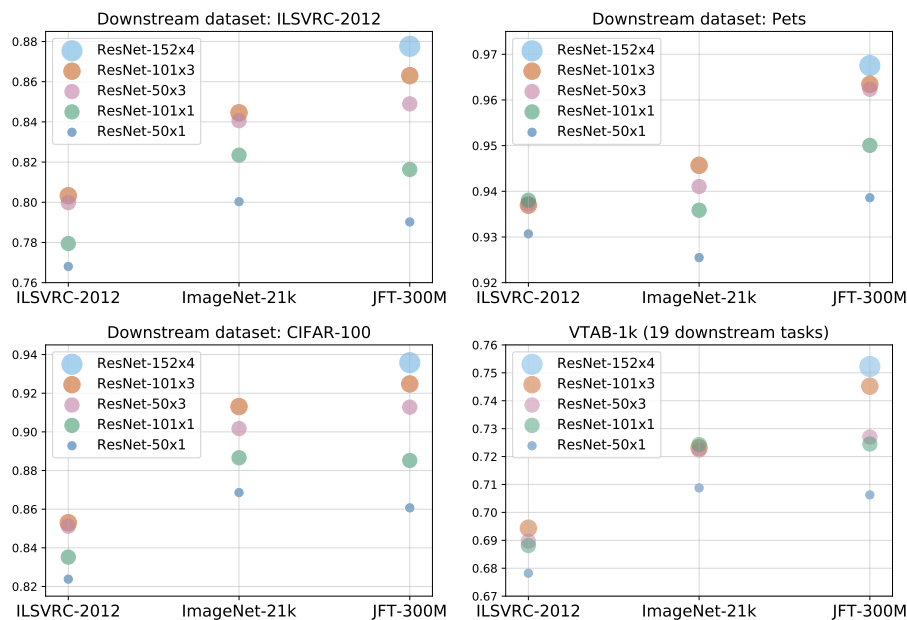


Fig. 4: Effect of upstream dataset (denoted on the x-axis) and model size on downstream performance.

architectures on three upstream datasets: ILSVRC-2012, ImageNet-21k and JFT-300M, and evaluate them on four downstream benchmarks (Figure 4). We opt for training the following models that have different capacity: ResNet-50x1, ResNet-50x3, ResNet-101x1, and ResNet-101x3. For the largest dataset, JFT-300M, we also train an extra large ResNet-152x4 model.

The gain from using large models is much more pronounced when pre-training on larger datasets. When pre-training on ILSVRC-2012, the benefit from larger models is significant, but quickly diminishes. However, improvements from scaling up the architecture are much more pronounced for larger datasets, such as ImageNet-21k or JFT-300M. A similar effect is observed when training on Instagram hashtags [31].

There is a second effect: not only is there limited benefit of training a large model on a small dataset, but there is also limited (or even negative) benefit from training a small model on a large dataset. Interestingly, the ResNet-50x1 model trained on the JFT-300M dataset performs worse or similar to the same architecture trained on the much smaller ImageNet-21k dataset. Thus, if one employs only architectures with usual capacity, one may conclude that scaling up data size does not bring any additional benefits. However, with larger architectures, such as ResNet-101x3, models pre-trained on JFT-300M significantly outperform those pre-trained on ILSVRC-2012 or ImageNet-21k.

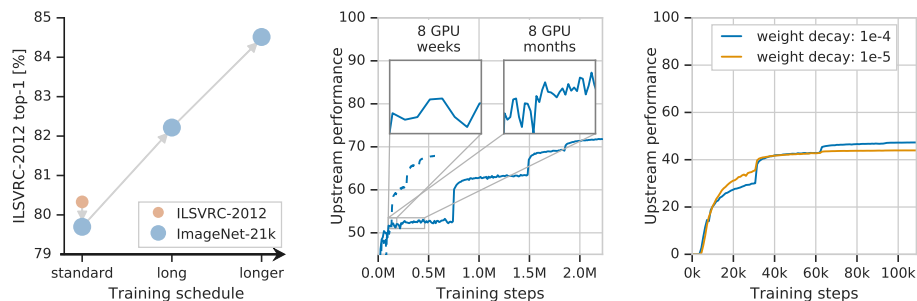


Fig. 5: Upstream training caveats, see Section 4.2 for details. **Left:** Applying the “standard” computational budget of ILSVRC-2012 to the larger ImageNet-21k seems detrimental - only when we train longer do we start seeing the benefit of training on the larger dataset. **Middle:** The learning progress of a ResNet-101x3 on JFT-300M seems to be flat even after 8 GPU-weeks, but after 8 GPU-months progress is clear. If one decays the learning rate too early (dashed curve), final performance is significantly worse. **Right:** Faster initial convergence with lower weight decay may trick the practitioner into selecting a suboptimal value. Higher weight decay looks worse initially, but results in a better final model.

Crucially, we also observe that large pre-trained models lead to improved results even on small downstream datasets. On VTAB-1k, which measures the average accuracy across 19 tasks with only 1000 training samples per task (Figure 4, lower right corner), the largest models also result in the best performance. It seems remarkable that it is not only possible to fine-tune such large models using comparatively little data, but that it leads to strong results.

4.2 Optimization on Large Datasets

For standard computer vision datasets such as ILSVRC-2012, there are well-known training procedures that are robust and lead to good performance. Progress in high-performance computing has made it feasible to learn from much larger datasets, such as ImageNet-21k, which has 14.2M images compared to ILSVRC-2012’s 1.28M. However, there are no established procedures for training from such large datasets. This section aims to tackle this shortcoming and provide pointers for training models on large datasets.

We first note that sufficient computational budget is crucial for training performant models on large datasets. The standard ILSVRC-2012 training schedule processes roughly 100 million images (1.28M images \times 90 epochs). However, if the same computational budget is applied to ImageNet-21k, the resulting model leads to worse performance on the ILSVRC-2012 validation set (Figure 5, bottom-left section of the leftmost plot). Nevertheless, as shown in the same figure, by increasing the computational budget, we not only recover ILSVRC-2012 performance, but significantly outperform it (we increased computational

Table 4: Top-1 accuracy of ResNet-50 on ILSVRC-2012 with a batch-size of 4096.

	Plain Conv	Weight Std.
Batch Norm.	75.6	75.8
Group Norm.	70.2	76.0

Table 5: Transfer performance of models from Table 4 on the 19 VTAB-1k tasks.

	Plain Conv	Weight Std.
Batch Norm.	67.72	66.78
Group Norm.	68.77	70.39

budget by factor 3 and 10 in the plot). Training with very large datasets such as JFT-300M may require extra patience. The validation error may not improve over a long time (Figure 5 middle plot, “8 GPU weeks” zoom-in), even though the model is still improving as evidenced by looking at a 4x longer time window.

Another important aspect of training with large datasets is the weight decay parameter. Lower weight decay can result in an apparent acceleration of convergence (Figure 5 rightmost plot, weight decay $1e-5$). However, this setting eventually results in an under-performing final model. This counter-intuitive behavior stems from the interaction of weight decay and normalization layers [26,28]. Low weight decay results in growing weight norms, which in turn results in a diminishing effective learning rate. Initially this effect creates an impression of faster convergence, but it eventually prevents further progress. A sufficiently large weight decay is required to avoid this effect. Throughout the paper, for upstream training, we use the standard weight decay of 10^{-4} [13,14].

Finally, we note that in all of our experiments we use stochastic gradient descent with momentum without any modifications. This is because, in our preliminary experiments, we did not observe clear benefits from using more involved adaptive gradient methods during upstream training.

4.3 Large Batches, Group Normalization and Weight Standardization

Currently, training on large datasets is only feasible using many hardware accelerators. Data parallelism is the most popular distributions strategy, and this naturally entails large batch sizes. Many known algorithms for training with large batch sizes use Batch Normalization (BN) [19] as a component [10] or even highlight it as the key instrument required for large batch training [7].

We also want to train large models, see Section 4.1. This significantly increases the memory requirement for any single accelerator chip, which necessitates small per-device batch sizes. However, it is known that models using BN perform worse when the number of images on each accelerator is too low [18]. An alternative strategy is to accumulate BN statistics across all of the accelerators. However, this strategy has two major drawbacks. First, computing BN statistics across large batches has been shown to harm generalization [7]. Second, using global BN requires many aggregations across accelerators which incurs significant latency.

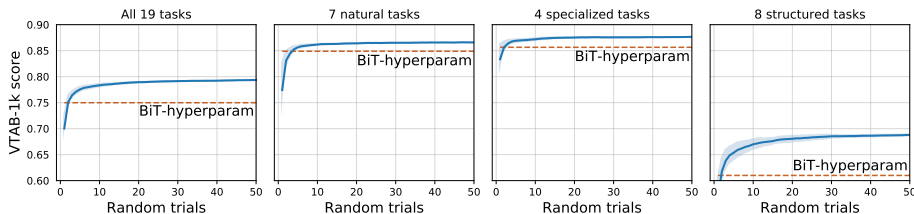


Fig. 6: VTAB-1k score (mean accuracy across tasks) depending on the total number of random hyperparameters tested. Depicted curves are averaged over 100 random hyperparameter orderings, and the shaded blue area indicates the standard error.

We therefore investigated alternatives to BN in ResNets, specifically Group Normalization (GN) [49] and Weight Standardization (WS) [36]. In our experiments we observe that combining GN and WN standardization recovers BN generalization performance and is stable when used for training with large input batches.

We investigated how these methods scale when using 128 accelerator chips and a batch size of 4096. We find that GN alone does not scale well to such large batches. We observe a performance drop of 5.4% on ILSVRC-2012 top-1 accuracy when using GN compared to using BN with a ResNet-50x1. However, the addition of WS enables GN to scale to such large batches, even outperforming BN. Table 4 summarizes these results.

We are not only interested in upstream performance, but also how models trained with GN and WS transfer. We transferred models with different combinations of BN, GN, and WS pre-trained on ILSVRC-2012 to the 19 tasks defined by VTAB-1k. Table 5 summarizes our results, which indicate that the GN and WS combination transfers significantly better than BN. We therefore use GN and WS in all of our BiT models.

4.4 Tuning hyperparameters for transfer

Throughout the paper we evaluate BiT using BiT-hyperparam. Here, we investigate whether BiT-L would benefit from additional computational budget for selecting fine-tuning hyperparameters.

For this investigation we use VTAB-1k as it contains a diverse set of 19 tasks. For each task we fine-tune BiT-L 50 times. Each trial uses randomly sampled hyperparameters, such as learning rate, number of updates and dropout rate for the penultimate layer. The full search space is provided in Appendix A. We select the best model for each dataset using the validation set and report results on the test set.

Overall, our random search improves performance over BiT-hyperparam on VTAB-1k by 4.5%. Figure 6 shows how VTAB performance improves with the

Table 6: Performance of BiT-L on the original (“Full”) and deduplicated (“Dedup”) test data. The “Dups” column shows the total number of near-duplicates found.

	From JFT			From ImageNet21k			From ILSVRC-2012		
	Full	Dedup	Dups	Full	Dedup	Dups	Full	Dedup	Dups
ILSVRC-2012	87.8	87.9	6470	84.5	85.3	3834	80.3	81.3	879
CIFAR-10	99.4	99.3	435	98.5	98.4	687	97.2	97.2	82
CIFAR-100	93.6	93.4	491	91.2	90.7	890	85.3	85.2	136
Pets	96.8	96.4	600	94.6	94.5	80	93.7	93.6	58
Flowers	99.7	99.7	412	99.5	99.5	335	91.0	91.0	0

number of random hyperparameter trials. We show mean accuracy across all 19 tasks from VTAB and the mean accuracy across each group of VTAB tasks. Since the order in which we pick the hyperparameters matters, we generate 100 random orderings of our hyperparameter trials and report average performance over these orderings. The standard error is shown as a shaded blue region around the mean.

Surprisingly, we conclude that with 10 to 20 hyperparameter trials, nearly optimal results can already be achieved. This means that if a practitioner wants to achieve the best possible score on their dataset, they will likely require only a modest computational budget for hyperparameter search.

4.5 Duplicates and near-duplicates

In order to make sure that our results are not inflated due to overlap between upstream training and downstream test data, we run extensive de-duplication experiments. For each upstream training dataset (JFT-300M, ImageNet-21k, and ILSVRC-2012) we remove all near-duplicates from our evaluation test sets and re-evaluate the best model on the de-duplicated test sets. The results are shown in Table 6: “Full” is the accuracy on the original test set, “Dedup” is the accuracy on the test set without near-duplicates, and “Dups” is the number of near-duplicates that have been removed. We observe that near-duplicates barely affect our results, so we report the results on the full test sets throughout the paper for comparability to previously published results. Note that near-duplicates between training and test sets have previously been reported by [40] for ILSVRC-2012, and by [3] for CIFAR.

In Section D in the appendix we present a few duplicates found between the ILSVRC-2012 training set and our downstream datasets.

5 Related Work

Large-scale Weakly Supervised Learning of Representations A number of prior works use large supervised datasets for pre-training visual representa-

tions [21,40,27,31]. In [21,27] the authors use a dataset containing 100M Flickr images [44]. This dataset appears to transfer less well than JFT-300M, which could be due to the limited domain of the data, noise in the text annotations, or architectures used. In [40], authors train on JFT-300M. This paper focuses on the effect of dataset size, and shows that transfer performance increases when using this large dataset, despite reporting a large degree of noise (20% precision errors) in the JFT-300M labels. An even larger labelled dataset of 3.5B Instagram images is used in [31]. The labels consist of noisy user-generated hashtags. A stronger ILSVRC-2012 performance of 85.4% is reported in [31], compared to 79.2% in [40]. The authors claim that the improvement is due to the larger dataset and better architecture (ResNeXt [51]). We show that we can attain better performance again with ResNet on the JFT-300M dataset using appropriate adjustments presented in Section 2. These papers focus on transfer to ImageNet classification, and COCO or VOC detection and segmentation. We show that transfer is also highly effective in the low data regime, and also works well on the broader set of 19 datasets in VTAB [55].

Specialized Representations Rather than pre-train generic representations, recent works have shown strong performance by training task-specific representations [52,33,50]. These papers condition on a particular task when training on a large support dataset. [52,50] train student networks on a large unlabelled support dataset using the predictions of a teacher network trained on the target task. [33] compute importance weights on the a labelled support dataset by conditioning on the target dataset. They then train the representations on the re-weighted source data. Even though these approaches may lead to superior results, they require knowing the downstream dataset in advance and substantial computational resources for each downstream dataset.

Unsupervised and Semi-Supervised Representation learning Self-supervised methods have shown the ability to leverage unsupervised datasets to transfer to labelled tasks. For example, [11] show that unsupervised representations trained on 1B unlabelled Instagram images transfer comparably or better than supervised ImageNet features to COCO, VOC, LVIS, and Cityscapes detection and segmentation. Semi-supervised learning exploits unsupervised data drawn from the same domain as the labelled data. [4] used self-supervised learning to attain strong performance on CIFAR-10 and SVHN using only 250 labels. Recent works combine self-supervised and semi-supervised learning to attain good performance with fewer labels on ImageNet [54,15]. [55] study many representation learning algorithms — unsupervised, semi-supervised, and supervised — and evaluate their representation’s ability to generalize to novel tasks. This paper shows that a combination of supervised and self-supervised representations works best. However, all models evaluated in that paper were trained on ILSVRC-2012. We show that supervised pre-training on larger datasets continues to be effective on diverse tasks.

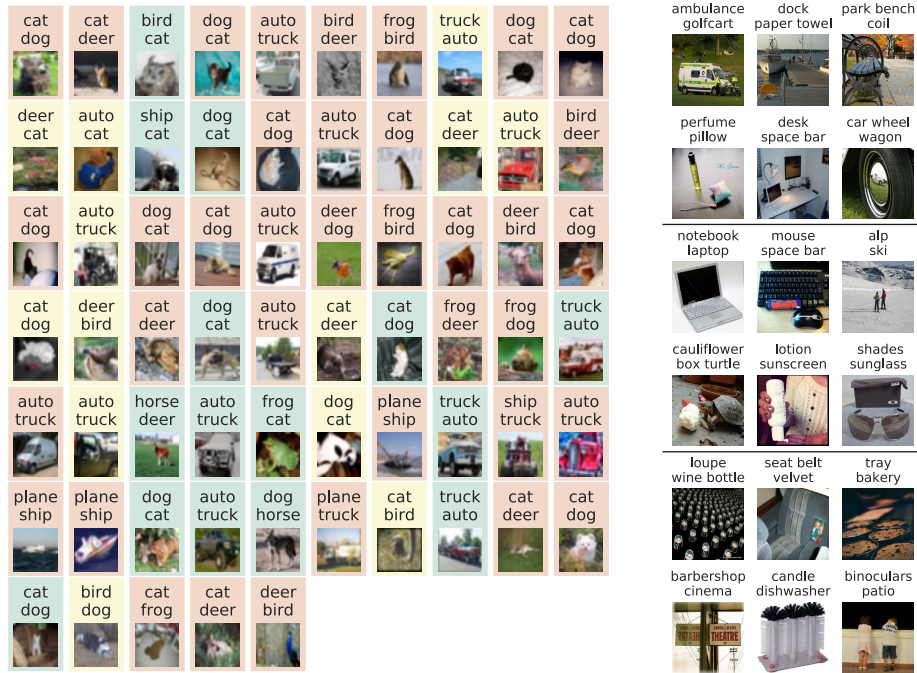


Fig. 7: Cases where the model’s predictions (top word) do not match the ground-truth labels (bottom word), and hence are counted as top-1 errors. **Left:** All of BiT-L’s mistakes on CIFAR-10, colored by whether five human raters agreed with BiT-L’s prediction on top (green), agreed with the ground-truth label on the bottom (red) or were unsure or disagreed with both labels (yellow). **Right:** Selected representative mistakes of BiT-L on ILSVRC-2012. Top group: The model’s prediction is more representative of the primary object than the label. Middle group: According to top-1 accuracy the model is incorrect, but according to top-5 it is correct. Bottom group: The model’s top-10 predictions are incorrect.

Few-shot Learning Many strategies have been proposed to attain good performance when faced with novel classes, and that use only a few examples per class. Meta-learning or metric-learning techniques have been proposed to learn with few or no labels, such as [48,39,41]. However, recent papers have shown that a simple linear classifier on top of pre-trained representations or fine-tuning can attain similar or better performance [5,32]. The upstream pre-training and downstream few-shot learning are usually performed on the same domain, with disjoint class labels. Our goal is to find a generalist representation which works well when transferring to many downstream tasks. Thus we do not force classes to be disjoint during train and test, but rather focus on the effectiveness of transferring general representations to many downstream tasks from multiple domains.

6 Discussion

We have revisited classical transfer learning, where a large pre-trained generalist model is fine-tuned to downstream tasks. We provide a simple recipe which exploits large scale pre-training to yield good performance on all of these tasks. BiT uses a clean training and fine-tuning setup, with a small number of carefully selected components, to balance complexity and performance.

Figure 7 shows all of BiT-L’s mistakes on CIFAR-10, and some examples from ILSVRC-2012. Visualizing these mistakes, we can see that many of these label/prediction mismatches are not true ‘mistakes’. In many cases, the model’s classification is valid — but it does not match the label. For example, the model may identify another prominent object when there are multiple objects in the image, or may provide an valid classification when the main entity has multiple attributes. There are some cases of label noise, where the model’s prediction is a better fit than the ground-truth label. In Figure 7 we can see that around half of the model’s mistakes on CIFAR-10 are due to ambiguity or label noise. We illustrate mistakes for more downstream datasets in Appendix C. Overall, by inspecting the mistakes we observe that performance on the standard vision benchmarks seems to have approached a saturation point.

We therefore also explore the effectiveness of transfer to two classes of more challenging tasks: classical tasks, but with very few labels to adapt to the new domain, and VTAB, which contains more diverse tasks, such as spatial localization, tasks from simulated environments, and medical imaging tasks. These benchmarks are much further from saturation, and BiT-L yields strong performance on both.

In the future we plan to further investigate transfer learning in the low data regime and look deeper into non-standard computer vision tasks, which pose new challenges and require holistic image understanding.

References

1. Athiwaratkun, B., Finzi, M., Izmailov, P., Wilson, A.G.: There are many consistent explanations of unlabeled data: Why you should average. In: ICLR (2019)
2. Ba, J.L., Kiros, J.R., Hinton, G.E.: Layer normalization. arXiv preprint arXiv:1607.06450 (2016)
3. Barz, B., Denzler, J.: Do we train on test data? purging CIFAR of near-duplicates. CoRR (2019), <http://arxiv.org/abs/1902.00423>
4. Berthelot, D., Carlini, N., Cubuk, E.D., Kurakin, A., Sohn, K., Zhang, H., Rafel, C.: ReMixMatch: Semi-supervised learning with distribution alignment and augmentation anchoring. arXiv preprint arXiv:1911.09785 (2019)
5. Chen, W., Liu, Y., Kira, Z., Wang, Y.F., Huang, J.: A closer look at few-shot classification. In: ICLR (2019)
6. Chollet, F.: Xception: Deep learning with depthwise separable convolutions. In: CVPR (2017)
7. De, S., Smith, S.L.: Batch normalization has multiple benefits: An empirical study on residual networks (2020), <https://openreview.net/forum?id=BJeVklHtPr>

8. Deng, J., Dong, W., Socher, R., Li, L.J., Li, K., Fei-Fei, L.: Imagenet: A large-scale hierarchical image database. In: CVPR (2009)
9. Goyal, P., Dollár, P., Girshick, R., Noordhuis, P., Wesolowski, L., Kyrola, A., Tulloch, A., Jia, Y., He, K.: Accurate, large minibatch sgd: training imagenet in 1 hour. arXiv preprint arXiv:1706.02677 (2017)
10. Goyal, P., Dollár, P., Girshick, R.B., Noordhuis, P., Wesolowski, L., Kyrola, A., Tulloch, A., Jia, Y., He, K.: Accurate, large minibatch sgd: Training imagenet in 1 hour. ArXiv **abs/1706.02677** (2017)
11. He, K., Fan, H., Wu, Y., Xie, S., Girshick, R.: Momentum contrast for unsupervised visual representation learning. arXiv preprint arXiv:1911.05722 (2019)
12. He, K., Girshick, R., Dollár, P.: Rethinking imagenet pre-training. In: ICCV (2019)
13. He, K., Zhang, X., Ren, S., Sun, J.: Deep residual learning for image recognition. In: CVPR (2016)
14. He, K., Zhang, X., Ren, S., Sun, J.: Identity mappings in deep residual networks. In: ECCV (2016)
15. Hénaff, O.J., Razavi, A., Doersch, C., Eslami, S., Oord, A.v.d.: Data-efficient image recognition with contrastive predictive coding. arXiv preprint arXiv:1905.09272 (2019)
16. Hinton, G., Vinyals, O., Dean, J.: Distilling the knowledge in a neural network. arXiv preprint arXiv:1503.02531 (2015)
17. Huang, Y., Cheng, Y., Chen, D., Lee, H., Ngiam, J., Le, Q.V., Chen, Z.: GPipe: Efficient training of giant neural networks using pipeline parallelism. arXiv preprint arXiv:1811.06965 (2018)
18. Ioffe, S.: Batch renormalization: Towards reducing minibatch dependence in batch-normalized models. In: NIPS (2017)
19. Ioffe, S., Szegedy, C.: Batch normalization: Accelerating deep network training by reducing internal covariate shift. ICML (2015)
20. Izmailov, P., Podoprikin, D., Garipov, T., Vetrov, D., Wilson, A.G.: Averaging weights leads to wider optima and better generalization. arXiv preprint arXiv:1803.05407 (2018)
21. Joulin, A., van der Maaten, L., Jabri, A., Vasilache, N.: Learning visual features from large weakly supervised data. In: ECCV (2016)
22. Jouppi, N.P., Young, C., Patil, N., Patterson, D., Agrawal, G., Bajwa, R., Bates, S., Bhatia, S., Boden, N., Borchers, A., et al.: In-datacenter performance analysis of a tensor processing unit. In: International Symposium on Computer Architecture (ISCA) (2017)
23. Kingma, D.P., Ba, J.: Adam: A method for stochastic optimization. arXiv preprint arXiv:1412.6980 (2014)
24. Kornblith, S., Shlens, J., Le, Q.V.: Do better imagenet models transfer better? CVPR (2019)
25. Krizhevsky, A.: Learning multiple layers of features from tiny images. Tech. rep. (2009)
26. van Laarhoven, T.: L2 regularization versus batch and weight normalization. CoRR (2017)
27. Li, A., Jabri, A., Joulin, A., van der Maaten, L.: Learning visual n-grams from web data. In: ICCV (2017)
28. Li, Z., Arora, S.: An exponential learning rate schedule for deep learning. arXiv preprint arXiv:1910.07454 (2019)
29. Lin, T.Y., Maire, M., Belongie, S., Hays, J., Perona, P., Ramanan, D., Dollár, P., Zitnick, C.L.: Microsoft COCO: Common objects in context. In: ECCV (2014)

30. Loshchilov, I., Hutter, F.: Sgdr: Stochastic gradient descent with warm restarts. arXiv preprint arXiv:1608.03983 (2016)
31. Mahajan, D., Girshick, R., Ramanathan, V., He, K., Paluri, M., Li, Y., Bharambe, A., van der Maaten, L.: Exploring the limits of weakly supervised pretraining. In: ECCV (2018)
32. Nakamura, A., Harada, T.: Revisiting fine-tuning for few-shot learning. arXiv preprint arXiv:1910.00216 (2019)
33. Ngiam, J., Peng, D., Vasudevan, V., Kornblith, S., Le, Q.V., Pang, R.: Domain adaptive transfer learning with specialist models. arXiv preprint arXiv:1811.07056 (2018)
34. Nilsback, M.E., Zisserman, A.: Automated flower classification over a large number of classes. In: Indian Conference on Computer Vision, Graphics and Image Processing (2008)
35. Parkhi, O.M., Vedaldi, A., Zisserman, A., Jawahar, C.V.: Cats and dogs. In: CVPR (2012)
36. Qiao, S., Wang, H., Liu, C., Shen, W., Yuille, A.: Weight standardization. arXiv preprint arXiv:1903.10520 (2019)
37. Raghu, M., Zhang, C., Kleinberg, J., Bengio, S.: Transfusion: Understanding transfer learning with applications to medical imaging. arXiv preprint arXiv:1902.07208 (2019)
38. Russakovsky, O., Deng, J., Su, H., Krause, J., Satheesh, S., Ma, S., Huang, Z., Karpathy, A., Khosla, A., Bernstein, M., Berg, A.C., Fei-Fei, L.: ImageNet Large Scale Visual Recognition Challenge. IJCV (2015)
39. Snell, J., Swersky, K., Zemel, R.: Prototypical networks for few-shot learning. In: NIPS (2017)
40. Sun, C., Shrivastava, A., Singh, S., Gupta, A.: Revisiting unreasonable effectiveness of data in deep learning era. In: ICCV (2017)
41. Sung, F., Yang, Y., Zhang, L., Xiang, T., Torr, P.H., Hospedales, T.M.: Learning to compare: Relation network for few-shot learning. In: CVPR (2018)
42. Szegedy, C., Vanhoucke, V., Ioffe, S., Shlens, J., Wojna, Z.: Rethinking the inception architecture for computer vision. In: CVPR (2016)
43. Tan, M., Le, Q.: Efficientnet: Rethinking model scaling for convolutional neural networks. In: ICML (2019)
44. Thomee, B., Shamma, D.A., Friedland, G., Elizalde, B., Ni, K., Poland, D., Borth, D., Li, L.J.: Yfcc100m: The new data in multimedia research. arXiv preprint arXiv:1503.01817 (2015)
45. Touvron, H., Vedaldi, A., Douze, M., Jégou, H.: Fixing the train-test resolution discrepancy. In: NeurIPS (2019)
46. Tschannen, M., Djolonga, J., Ritter, M., Mahendran, A., Houlsby, N., Gelly, S., Lucic, M.: Self-supervised learning of video-induced visual invariances (2019)
47. Ulyanov, D., Vedaldi, A., Lempitsky, V.: Instance normalization: The missing ingredient for fast stylization. arXiv preprint arXiv:1607.08022 (2016)
48. Vinyals, O., Blundell, C., Lillicrap, T., Wierstra, D., et al.: Matching networks for one shot learning. In: NIPS (2016)
49. Wu, Y., He, K.: Group normalization. In: ECCV (2018)
50. Xie, Q., Hovy, E., Luong, M.T., Le, Q.V.: Self-training with noisy student improves imagenet classification. arXiv preprint arXiv:1911.04252 (2019)
51. Xie, S., Girshick, R., Dollár, P., Tu, Z., He, K.: Aggregated residual transformations for deep neural networks. In: CVPR (2017)
52. Yalniz, I.Z., Jégou, H., Chen, K., Paluri, M., Mahajan, D.: Billion-scale semi-supervised learning for image classification. arXiv preprint arXiv:1905.00546 (2019)

53. Yun, S., Han, D., Oh, S.J., Chun, S., Choe, J., Yoo, Y.: Cutmix: Regularization strategy to train strong classifiers with localizable features. arXiv preprint arXiv:1905.04899 (2019)
54. Zhai, X., Oliver, A., Kolesnikov, A., Beyer, L.: S⁴L: Self-Supervised Semi-Supervised Learning. In: ICCV (2019)
55. Zhai, X., Puigcerver, J., Kolesnikov, A., Ruysen, P., Riquelme, C., Lucic, M., Djolonga, J., Pinto, A.S., Neumann, M., Dosovitskiy, A., et al.: The visual task adaptation benchmark. arXiv preprint arXiv:1910.04867 (2019)
56. Zhang, H., Cisse, M., Dauphin, Y.N., Lopez-Paz, D.: mixup: Beyond empirical risk minimization. In: ICLR (2017)

A Hyperparameters for random search

In Section 4.4 we use random hyperparameter search for analysis of performance headroom. Our random search includes following hyperparameters with the following ranges and sampling strategies:

- Initial learning rate is sampled log-uniformly from the range $[10^{-1}, 10^{-4}]$.
- Total number of updates is sampled from the set $\{500, 1000, 2000, 4000, 8000, 16000\}$.
- Dropout rate for the penultimate layer is uniformly sampled from the range $[0.0, 0.7]$.
- Weight decay to the initial weight values is sampled log-uniformly from the range $[10^{-1}, 10^{-6}]$.
- MixUp α parameter is sampled from the set $\{\text{None}, 0.05, 0.1, 0.2, 0.4\}$.
- Input image resolution is sampled from the set $\{64, 128, 192, 256, 320, 384\}$.

B Horizontal flipping and cropping for VTAB-1k tasks

When fine-tuning BiT models, we apply random horizontal flipping and cropping as image augmentations. However, these operations are not reasonable for certain VTAB tasks, where the semantic label (e.g. angle, location or object count) is not invariant to these operations.

Thus, we disable random horizontal flipping as preprocessing for dSprites/orientation, SmallNORB/azimuth and dSprites/location tasks. Random cropping preprocessing is disabled for Clevr/count, Clevr/distance, DMLab, KITTI/distance and dSprites/location tasks.

C All of BiT-L’s Mistakes

Here we show all mistakes made by BiT-L for Pets, Flowers and CIFAR-10. As in the main paper, the upper word shows the model’s prediction, while the lower word shows the ground-truth label. CIFAR-10 mistakes are shown in the main paper and are thus omitted here. The larger panels are best viewed on screen, where they can be magnified.

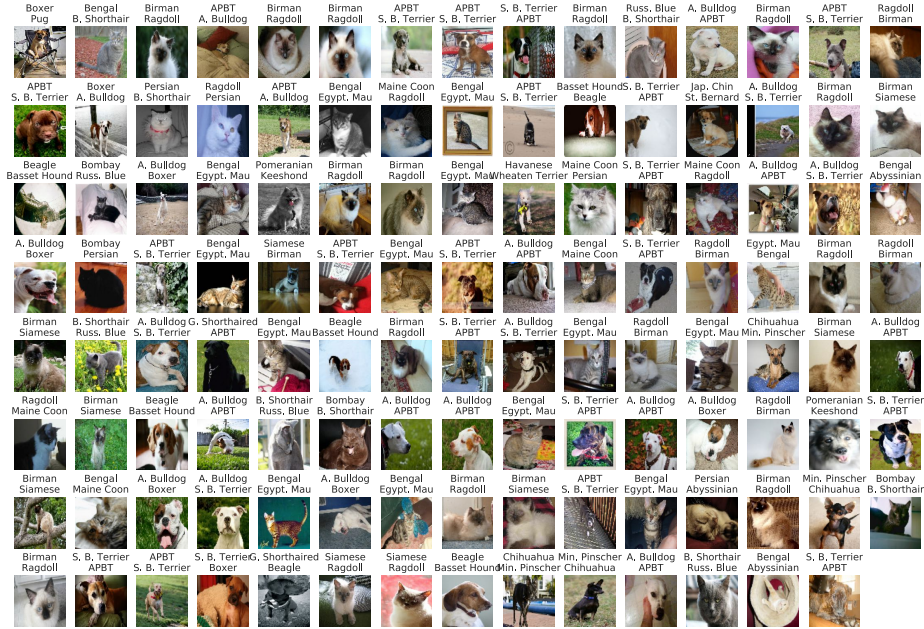


Fig. 8: All of BiT-L's 119 mistakes on Oxford-IIIT-Pet.



Fig. 9: All of BiT-L's 19 mistakes on Oxford-Flowers102.

D Duplicates and near-duplicates

Here (Figure 10) we present a few duplicates found between the ILSVRC-2012 training set and test splits of four standard downstream datasets. Details are in section 4.5 of the main text.

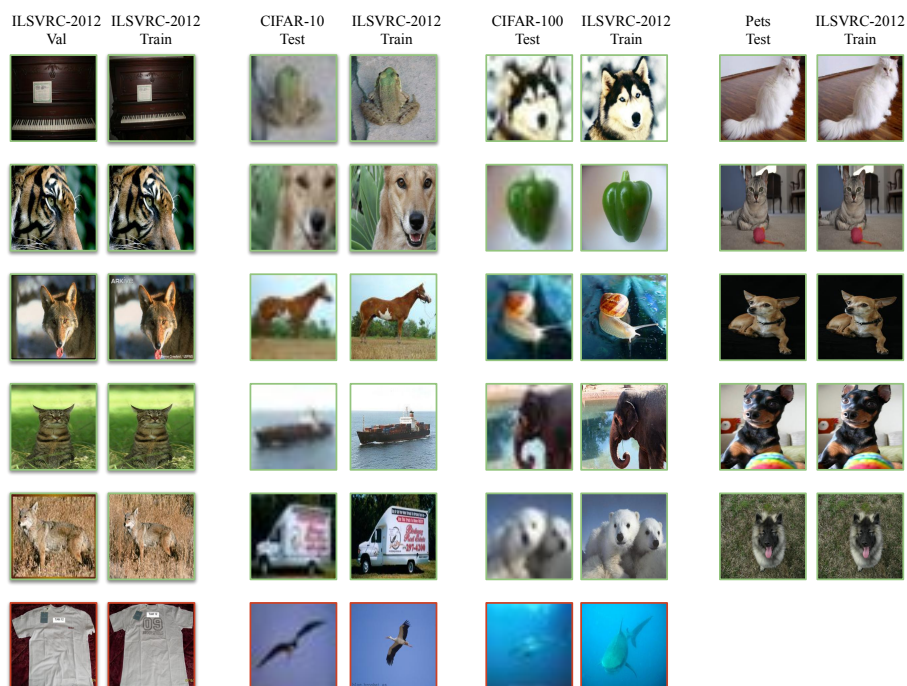


Fig. 10: Detected duplicates between the ILSVRC-2012 training set and test splits of various downstream datasets. Note that Flowers is not listed because there are no duplicates. Green borders mark true positives and red borders mark rare false positives.